Article:
Yao, F-Z, Wang, K, Jo, W et al. (8 more authors) (2016) Diffused Phase Transition Boosts Thermal Stability of High-Performance Lead-Free Piezoelectrics. Advanced Functional Materials. ISSN 1616-301X

https://doi.org/10.1002/adfm.201504256

Diffused Phase Transition Boosts Thermal Stability of High-Performance Lead-Free Piezoelectrics

Fang-Zhou Yao, Ke Wang, Wook Jo, Kyle G. Webber, Timothy P. Comyn, Jing-Xuan Ding, Ben Xu, Li-Qian Cheng, Mu-Peng Zheng, Yu-Dong Hou, and Jing-Feng Li**

F.-Z. Yao, Prof. K. Wang, J.-X. Ding, Prof. B. Xu, Dr. L.-Q. Cheng, Prof. J.-F. Li
State Key Laboratory of New Ceramics and Fine Processing,
School of Materials Science and Engineering,
Tsinghua University,
Beijing 100084, China
E-mail:jingfeng@mail.tsinghua.edu.cn; wang-ke@mail.tsinghua.edu.cn

Prof. W. Jo
School of Materials Science and Engineering,
Ulsan National Institute of Science and Technology,
Ulsan 689-798, South Korea

Prof. K. G. Webber
Department of Materials Science,
University of Erlangen-Nürnberg,
Erlangen 91058, Germany

Prof. T. P. Comyn
Institute for Materials Research,
University of Leeds,
Leeds LS2 9JT, UK

Dr. M.-P. Zheng, Prof. Y.-D. Hou
Department of Materials Science and Engineering,
Beijing University of Technology,
Beijing 100124, China

Keywords: lead-free, piezoelectric, niobate, phase transition, temperature stability

Abstract:

High piezoelectricity of $(K,Na)NbO_3$ (KNN) lead-free materials benefits from a polymorphic phase transition (PPT) around room temperature, but its temperature sensitivity has been a bottleneck impeding their applications. We find that good thermal stability can be achieved in $CaZrO_3$-modified KNN lead-free piezoceramics, in which the normalized strain d_{33}* almost keeps constant from room temperature up to 140 ^{o}C. *In situ* synchrotron X-ray diffraction experiments combined with permitivity measurements disclose the occurrence of a new phase transformation under an electrical field, which extends the transition range between tetragonal and orthorhombic phases. It is revealed that such an electrically-enhanced diffused

polymorphic phase transition (EED-PPT) contributed to the boosted thermal stability of KNN based lead-free piezoceramics with high piezoelectricity. The present approach based on phase engineering should also be effective in endowing other lead-free piezoelectrics with high piezoelectricity and good temperature stability.

1. Introduction

Piezoelectricity, a phenomenon whereby materials become electrically polarized upon the application of stress or deform in response to electrical stimuli, has been an active research topic since its discovery in 1880 by Pierre and Jacques Curie, because of its scientific interests and abundant applications. For the last half-century, the lead-contained materials, e.g., $Pb(Zr,Ti)O_3$ (PZT) and $Pb(Mg,Nb)O_3$-$PbTiO_3$ (PMN-PT), have been the icons of piezoelectrics, exhibiting a morphotropic phase boundary (MPB), where plural phases with negligible difference in free energy coexist and strongly enhanced functional properties arise.[1] However, a possible toxicity of lead in PZT and PMN-PT has been raising intense health and environmental concerns; thus, the last decade has witnessed the surging dedication to viable lead-free alternatives.[2-5] Resembling the principle characteristics of MPB,[4-10] polymorphic phase transition (PPT) boundary has also been extensively pursued.[2, 11, 12] Unfortunately, contrary to the nearly vertical MPB in the well-known PZT and PMN-PT systems,[1] the PPT in lead-free piezoelectrics is always tilted, resulting in unavoidable thermally unstable electromechanical properties.[13-15] Weak thermal stability is unacceptable for many industrial applications, even though lead-free piezoelectrics have competitive performance at ambient conditions. To address the issue, two approaches have been adopted so far, i.e., fabricating textured samples,[2] or shifting the PPT temperature $T_{O\text{-}T}$ well below room temperature.[13] However, the former confronts the poor reproducibility due to an excessively complex synthesis procedure; while the latter would inevitably sacrifice a large

portion of piezoelectric activity. Consequently, a barrier still exists in developing reliable lead-free piezomaterials as alternatives to currently market-dominating lead-based materials.

Inspired by the nature of MPB in PZT and PMN-PT with remarkable thermal stability, it has been considered that inducing an MPB or a diffused PPT in lead-free systems could be viable options.[16, 17] Unfortunately, it has turned out that an intense temperature sensitivity still remains in lead-free piezoceramics with an engineered MPB, which is mainly attributed to the increased polarization anisotropy and the energy barrier for polarization rotation deviating from MPB.[16, 17] Thus, making PPT diffused becomes a more attractive solution to the dilemma, though no experimental success has been witnessed yet. It should be clarified that the diffused PPT in this scenario refers to the occurrence of distinct ferroelectric phase transitions over a wide temperature range, resembling the diffused phase transition in relaxor ferroelectrics where polar nano-regions (PNRs) plays an important role.[18]

In this work, we demonstrate that introducing an electrically-enhanced diffused polymorphic phase transition (EED-PPT) between tetragonal and orthorhombic phases in $(K,Na)NbO_3$ (KNN)-based lead-free piezoelectrics is highly beneficial in achieving enhanced piezoelectric responses as well as thermal stability. First-principles calculations reveal that electrically-enhanced diffuseness in PPT originates from the fact that the two ferroelectric phases are energetically close to each other. Validation of the concept was exemplified in one of the most promising lead-free piezoelectrics, KNN with the nominal compositions of $(100-x)(Na_{0.49}K_{0.49}Li_{0.02})(Nb_{0.8}Ta_{0.2})O_3$-$xCaZrO_3$ (denoted by CZx).

2. Results and Discussion

The X-ray diffraction (XRD) patterns are presented in **Figure 1**(a), describing the materials as solid solutions with a perovskite structure. Tiny secondary phases are traced in the 2θ range from 20^o to 40^o, possibly because of the undesirable reactions between various species during the synthesis process resulting from complex constitution of the nominal composition. In

general, the phase structure of KNN-based ceramics can be quantified by assessing the relative intensities of (002) and (200) peaks (I_{002}/I_{200}).[19] The tetragonal phase has a theoretical ratio I_{002}/I_{200} of 1:2 and it is reciprocal for an orthorhombic phase. Compared with those of CZ0 and CZ6, the (002) and (200) profiles of as-sintered CZ5 ceramics are of comparable intensity and are also very close to each other (see the inset figure of Figure 1(a)), representing a pseudocubic perovskite structure with the coexistence of tetragonal and orthorhombic phases, which signifies promising piezoelectricity inherent in CZ5, the material of choice in this study.[20] In addition to the phase structure, the piezoelectric properties of ferroelectric polycrystals are also closely associated with domain morphologies.[21, 22] Representative domain configurations of CZ5 were revealed by transmission electron microscopy (TEM) and piezoresponse force microscopy (PFM) studies, as depicted in Figure 1(b). It is observed that stripe-like domains in nano-scale dominate in the polycrystals. Benefiting from the reduced domain wall energy, the nano-domains can easily respond to external excitations, e.g., mechanical force or electric field, contributing to the large piezoelectric performance.[23]

There are several methods to quantitatively determine piezoelectric responses, two of which used frequently are to collect the charge in response to mechanical stimuli or to normalize the electric field induced strain, known as piezoelectric coefficient d_{33} and normalized strain d_{33}* (unipolar strain output divided by the corresponding field), respectively. In this sense, the piezoelectric output is composed of intrinsic and extrinsic contributions. The former refers to linear piezoelectric effect derived from lattice displacement, whereas the latter is related to the dynamics of domain wall motions, which is largely influenced by the amplitude of input stimuli.[24] Due to the combined effects of PPT and nano-domain contribution as stated above, poled CZ5 ceramics exhibit superior piezoelectric performance at room temperature. The piezoelectric coefficient d_{33} reached 357 pCN^{-1}, which is among the top values for randomly-orientated KNN ceramics and is comparable to those of hard PZT[25]

and PMN-PT[26] ceramics prepared by conventional route, though outperformed by PMN-PT crystals.[27] Large unipolar strain output of 0.16 % was also obtained under an electric field of 6 $kVmm^{-1}$, accompanied by a small strain hysteresis (see Figure 1(c)), enabling the current material to be a promising potential for actuator applications. Nevertheless, excellent thermal stability of strain behavior is further demanded for successful implementations. Intriguingly, current material possesses nearly temperature-insensitive strain behavior up to 140 ^{o}C at an electric field of 5 $kVmm^{-1}$, the variation of which in the investigated temperature range is within $\pm$10 % of its room-temperature value, being much better than other lead-free systems and also being comparable to the classical PZT4 ceramics (refer to Figure 1(d)).[2, 28-30]

To uncover the underlying mechanism, herein, we focus on the influence of external electric field on the temperature stability of d_{33}*. The temperature dependence of normalized d_{33}* under different electric fields are summarized in **Figure 2**(a). At a very small field (0.01 $kVmm^{-1}$), the d_{33}* peaks at 36 ^{o}C and decreases dramatically when temperature rises, justified by the fading of ferroelectric domain contrasts (shown in **Figure 3**) as well as the reduced lattice displacement[31] (refer to the evolution of (200) pseudocubic reflections with temperature in **Figure 4**). As outlined above, performance of piezoelectrics is strongly correlated with domain morphologies, particularly among which the nano-domains could extrinsically contribute to the enhanced piezoelectric properties.[21, 22] It is observed from the temperature-dependent domain evolution revealed by PFM in Figure 3(a-d) that the ferroelectric nano-domains gradually shrink as temperature approaches the Curie point T_C. The absence of nano-domains at elevated temperatures was also reported in KNN by hot-stage TEM.[32] The insets in Figure 3(a-d) correspond to the histograms of PFM phase images, where the peaks demonstrate the distribution of domains with distinct orientations. Both the histograms and line scan profiles in Figure 3(e-f) confirm the gradual depolarization process, i.e. loss of switchable polarization (or lattice displacement) at high temperature, as represented by the changes of polarization hysteresis and *in situ* synchrotron XRD patterns

with temperature (see Figure S2(b) and Figure 4, respectively). Thus, the severely depressed extrinsic contribution from domain wall motions and intrinsic counterpart from lattice displacement lead to the massive loss of small signal piezoelectric performance at high temperatures. Most interestingly, larger electric fields favor better temperature stability, while the peak of d_{33}* *versus* temperature plots shifts from 36 to 65 ^{o}C and transforms into a plateau with increasing sequence of field levels. Under an electric field of 5 kVmm^{-1}, desirable thermal stability was obtained; variation of d_{33}* maintains ± 10% of d_{33RT}* over a wide temperature range from ambient temperature to 140 ^{o}C.

For further understanding of the electric-field-dependent behaviors in CZ5, two parameters, PPT point $T_{O\text{-}T}$ and the range of PPT $T_{O\text{-}T}^{90\%}$ were introduced. The former is defined as the temperature where d_{33}* maximizes and corresponds to the commensurate content of each ferroelectric phase, while the latter is the temperature difference between the two points holding 90 % of the maximum value, assigned as the temperature range of PPT (see Figure S1). As depicted in Figure 2(b), the PPT point $T_{O\text{-}T}$ ascends linearly with the magnitude of external field, which could be rationalized by the Ginzburg-Landau-Devonshire (GLD) model.[33-36] For a stress-free single crystalline ferroelectric with a mono-domain state, the free energy G as a function of polarization P is written as the following polynomial:[33, 34] $G=\alpha\left(T-T_0\right)P^2+\beta P^4+rP^6$, where α, β, γ and T_0 are material-dependent constants and the Curie-Weiss temperature, respectively. The derivative of G with respect to P yields a relationship between electric field E and P: $\frac{\partial G}{\partial P}=E=2\alpha(T-T_0)P+4\beta P^3+6\gamma P^5$ .In this case, T_0 can be taken as the PPT point $T_{O\text{-}T}$ under zero electric field, and it is reasonable to eliminate the high order terms as they are insignificant, resulting in a shortened formula of $E=2\alpha(T-T_0)P$. Thus, the PPT point $T_{O\text{-}T}$ as a function of electric field E can be derived: $T_{O\text{-}T}=\frac{1}{2\alpha P}E+T_0$, where the first term is the offset of PPT point $T_{O\text{-}T}$ induced by the electrical

poling. Fitting of experimental data within the range from 1 to 5 $kVmm^{-1}$ yields the magnitude of electric field dependence of $T_{O\text{-}T}$, $T_{O\text{-}T}=6E+35$, agreeing well with the GLD model. A predicted PPT point $T_{O\text{-}T}$ at zero field is obtained at T_0=35 ^oC, consistent with the experimental value of 36 ^oC determined from Figure 1(b). Being parallel to PPT point $T_{O\text{-}T}$, the range of PPT $T_{O\text{-}T}^{90\%}$ follows an ascending trend with increasing external fields. Analogous phenomenon of field induced broadening of the coexistence region was also observed in lead-based crystals, which was ascribed to the presence of polar nano-regions (PNRs) within the ferroelectric phases.[37]

Measurement of temperature-dependent dielectric properties is the most convenient and simple method to identify the phase transition temperatures of ferroelectrics at ambient conditions.[1, 4, 20] It was also performed in this study but with a special emphasis on the changes of dielectric properties with electric field excursion. Figure S2 presents the field-dependent permittivity curves at selected temperatures, from which dielectric constant as a function of temperature under external fields can be extracted, provided in Figure 2(c). Without electric field, an anomaly is observed around 50 ^oC, corresponding to the PPT point $T_{O\text{-}T}$. It should be mentioned that the field-dependent permittivity curves were collected in a heating cycle, and the intrinsic thermal hysteresis usually leads to a higher $T_{O\text{-}T}$ on an order of tens of degrees Celsius, i.e., $T_{O\text{-}T}$ should be located near room temperature. It is consistent with the direct permittivity measurement (see Fig. S3), where a Curie temperature T_C of 192 ^oC is recorded. However, when subjected to a large electric field, the peak in permittivity curve for CZ5 migrates towards higher temperature, accompanied by an apparent flattening, indicating the presence of phase transition induced by electric field. For the coercive field E_C, higher values can be recorded for ferroelectric phases at lower temperatures and it decreases linearly with increasing temperature in single-phase ferroelectrics. Therefore, E_C peaks close to the temperature range where polymorphic phases coexist. Coercive field E_C as a function of

temperature was determined by measuring polarization hysteresis at various temperatures, as shown in Figure 2(d). A dispersive peak of temperature-dependent coercive field E_C exists in the range from 0 to 100 ^oC, outside of which E_C declines monotonically, suggesting the extensive coexisting region of tetragonal and orthorhombic phases as well. All the above observations conformably uncover the fingerprints of electrically-enhanced diffused polymorphic phase transition (EED-PPT) in the KNN-based lead-free piezoceramics. Recently, nanoclusters are disclosed in an orthorhombic matrix of KNN ceramics.[38] Thus, the diffuseness of phase transition in present study may also originate from the existence of nanoscale regions in current material, resembling the case of relaxors.[37]

In situ synchrotron X-ray diffraction has been verified as a powerful protocol to resolve the structural puzzles in materials with complicated crystal structures, particularly in interpreting the role of external fields.[6, 39] Figure 4 displays the representative *in situ* synchrotron X-ray diffraction patterns, including the (111), (200), and (220) pseudocubic reflections under the combined effects of temperature and electric field. Upon the application of thermal and electrical stimuli, the diffraction profiles show visible changes, as depicted in Figure 4. Without applying external field, the phase structure of CZ5 evolves from coexisting tetragonal and orthorhombic phases to a single tetragonal phase with raising temperature up to 100 ^oC, and the c/a ratio (or the tetragonality) becomes smaller when further heating the samples. In addition to the intensity changes resulting from domain reorientation, the shifts of diffraction peak positions are also perceptible upon the application of an electric field, corresponding to the expansion or contraction in unit cell dimensions. Minor shift in peak position for (200) reflection was observed in the concerned temperature range (refer to the Figure S4 and Table S1). This phenomenon is not commensurate with the tetragonal model, where the peak position of (200) is immobile in typical tetragonal PZT regardless of the magnitude of external field.[6] It was further revealed that the piezoelectric elongation of the unit cells does not occur along the polar directions but along those directions associated with

the monoclinic distortion.[6] Based on the consistence between orthorhombic and monoclinic symmetries in KNN, namely, KNN has an orthorhombic structure in the context of crystallography while the perovskite ABO_3 primary cell possesses a monoclinic symmetry,[1, 19] the observations in present study can be attributed to the electric-field-induced phase transition from tetragonal to orthorhombic phase. Note that the diffraction profiles can switch back to the initial positions upon the removal of the poling field, implying a reversible nature of the electric-field-induced phase transition (refer to the 3D contour figures on the right panel in Figure 4).

As mentioned, the macroscopic piezoelectricity contains two basic ingredients, i.e., the intrinsic and extrinsic contributions.[24] Originating from domain wall motions, the extrinsic component is sensitive to frequency variation, whereas it does not influence the intrinsic part.[40] Previous works have revealed that extrinsic contribution plays an important role in KNN, especially for the compositions near PPT.[41, 42] Therefore, it provides us with another easy approach to locating the PPT point $T_{O\text{-}T}$ by assessing the temperature and frequency dependence of piezoelectric properties. **Figure 5** presents both the temperature and frequency dependent d_{33}* of CZ5 under various electric fields. The PPT point $T_{O\text{-}T}$, where d_{33}* maximizes, migrates towards higher values with increasing electric field at a given frequency, while d_{33}* declines, associated with reduced extrinsic contributions due to lagged domain wall motions at high frequencies.[40] However, the scenario of d_{33}* as functions of temperature and frequency is altered by the application of external field. Under a small electric field of 1 $kVmm^{-1}$, the d_{33}* is notably dependent on frequency at low temperatures (from 25 to 75^{o}C), but the trend is considerably weakened in a higher temperature range. When the electric field was raised up to 4 kV/mm^{-1}, the temperature range where d_{33}* is frequency-dependent, is significantly broadened, corresponding to an expanded PPT zone. It also finds consistence with the above analysis.

For a better understanding of the underlying mechanisms of enhanced performance in

piezoelectrics, the simple but classical $KNbO_3$ lead-free piezoelectric is recently highlighted in both theoretical and experimental researches.[3, 43] Considering that $KNbO_3$ follows an identical phase transition sequence with KNN-based ceramics, it is feasible to do fundamental first-principles calculations based on the prototype perovskite $KNbO_3$ to shed a light on the nature of phase transitions in KNN-based complex compositions. The calculated energy *versus* volume plots were summarized in **Figure 6**. It is observed that tetragonal and orthorhombic phases are equi-energetic but differ in volume, while the latter has a less compact structure, i.e., orthorhombic phase is more energetically favored compared to the tetragonal symmetry for $KNbO_3$ with a larger unit cell. Thus, phase transition from tetragonal to orthorhombic can be triggered if volume of unit cells gets expanded. For piezoelectrics, the real-time volume changes ΔV can be resolved by measuring the longitude strain S_{33} and transverse strain S_{11} simultaneously ($\Delta V = S_{33}+2S_{11}$).[28, 44] **Figure 7** shows the strain hysteresis with the concurrent electric-field-induced volume change ΔV of as-sintered CZ5 ceramics. The increasing ΔV demonstrates the expansion of unit cells when subjected to external fields, which favors the stabilization of orthorhombic phase as concluded from the first-principles calculations. No remnant ΔV is observed upon the removal of external field, indicating that the electric-field-induced volume change is reversible. It is consistent with the *in situ* synchrotron X-ray diffraction outcomes as presented in the previous section. The first-principles calculations, supported by the experimental determination of field-dependent volume change, unambiguously represent that it is possible to stabilize different polar phases by controlling the applied electric field[5, 6] in addition to the well-accepted approaches of composition,[1] stain,[9, 10] stress,[31] and pressure.[45] Note that KNN is not a unique system presenting energetically parallel phases; it is frequently observed in many perovskite piezoelectrics because of the flexibility of perovskite structure.[1, 4, 5] Therefore, the electric-field-induced phase transition and the associated tunable properties may occur in other

perovskite piezoelectric materials.

3. Conclusions

In this work, we revealed the origin of temperature-insensitive strain behaviors in a typical lead-free piezoelectric material by various techniques, such as *in situ* electrical measurements, domain evolution, and synchrotron X-ray diffraction profiles. First-principles calculations further augment the underlying mechanism as a diffused ferroelectric-to-ferroelectric phase transition intensified by increasing electric field. This finding provides a promising approach to enhance thermal stability of piezoelectricity by engineering polymorphic phase transition between two ferroelectric phases, mimicking the effect of a morphotropic phase boundary. Certainly, the present strategy is transferrable and would inspire plentiful researches on tailoring performance of other piezoelectrics by means of other intrinsic physical parameters, e.g., pressure and stress, as well as the analogous phenomena in parallel smart materials, such as ferromagnetics and ferroelastics, etc.

4. Experimental Section

Characterization of electrical properties, domain morphology, and phase structure: The CZx ceramics were prepared through a conventional solid state route as described elsewhere.[18] For macroscopic electrical characterizations, as-sintered ceramics were polished down to 1 mm in thickness and painted with silver pastes fired at 550 ^{o}C for 30 min to form electrodes. The samples were poled under an electric field of 4 kV mm^{-1} at 120 ^{o}C in silicone oil for 30 min. The piezoelectric coefficient d_{33} was measured using a quasi-static d_{33} meter (ZJ-3A, Institute of Acoustics, Chinese Academy of Science, Beijing, China) and also determined *in situ* as a function of temperature by a custom-designed apparatus. The polarization $P(E)$ hysteresis, unipolar piezoelectric strain $S(E)$, and permittivity $\varepsilon_{33}(E)$ curves were recorded by a ferroelectric tester (aixACCT TF Analyzer 1000, Germany). For $P(E)$ measurement, an

electric field of 3 kV mm^{-1} at 1 Hz was applied. The piezoelectric strain $S(E)$ curves were determined using a unipolar triangular-shaped electric field at a fixed frequency of 1 Hz. The small-signal field-dependent $\varepsilon_{33}(E)$ were measured by applying a triangular signal of 4 kV/mm and the frequency of 1 Hz, on which an AC voltage of 25 V and at 250 Hz was superimposed. To determine the volume change, three linear variable displacement transducers (LVDT) were used to measure the electric-field-induced strains; one for the longitudinal strain S_{33} in the thickness direction and two for the transverse strain S_{11} in the radial direction. For the PFM observations, as-sintered samples were mechanically polished to about 20 μm in thickness. The PFM experiments were carried out using a commercial atomic force microscopy (MFP-3D, Asylum Research, USA). The PFM signal was recorded at room temperature under ac voltage U_{ac}=5-10 V, f_{ac}=50 kHz applied to a conductive Pt-Ir coated cantilever PPP-NCHPt (Nanosensors, Switzerland). *In situ* evolution of domain configuration with temperature at the range from 25 to 150 ^{o}C was also studied using PFM. To overcome the issue of image drift as a result of thermal expansion of samples and probes at high temperatures, larger area will be scanned to locate the desired region precisely after the sample is heated to a certain temperature and reaches a stable state. And then, it is necessary to retune the resonant frequency in case of frequency shift at increased temperatures. Afterwards, reliable temperature-dependent PFM images can be acquired. Influence of thermal and field stimuli on *in situ* synchrotron X-ray diffraction (XRD) profiles was evaluated at the Diamond Light Source, with an incident wavelength of 0.2189 Å.

First-principles calculations: First-principles calculations were performed on the prototype niobate perovskite $KNbO_3$ with different symmetries by using the density functional theory methods encoded in the Vienna *ab initio* Simulation Package.[46] General gradient approximation of Perdew, Burke, and Emzerhof form was adopted to estimate the exchange-correlation energy.[47] The projector augmented wave pseudopotentials were employed, as alternatives for the all-electron ion potentials.[48] The plane-wave energy was cut off by

500 eV and a Monkhorst-Pack mesh was used to sample the Brillouin zone. An energy convergence criterion of 10^{-8} eV was applied to all the calculations.

Supporting Information
Supporting Information is available from the Wiley Online Library or from the author.

Acknowledgements
This work was supported by National Nature Science Foundation of China (Grants no. 51332002, 51302144, 51221291) and the Ministry of Science and Technology of China under the Grant 2015CB654605.

Received:
Revised:
Published online:

[1] B. Jaffe, W. R. Cook and H. Jaffe, *Piezoelectric Ceramics*, Academic Press, London, UK **1971**.
[2] Y. Saito, H. Takao, T. Tani, T. Nonoyama, K. Takatori, T. Homma, T. Nagaya and M. Nakamura, *Nature* **2004**, 432, 84.
[3] T. T. Lummen, Y. Gu, J. Wang, S. Lei, F. Xue, A. Kumar, A. T. Barnes, E. Barnes, S. Denev, A. Belianinov, M. Holt, A. N. Morozovska, S. V. Kalinin, L. Q. Chen and V. Gopalan, *Nat. Commun.* **2014**, 5, 3172.
[4] W. Liu and X. Ren, *Phys. Rev. Lett.* **2009**, 103, 257602
[5] C. Ma, H. Guo, S. P. Beckman and X. Tan, *Phys. Rev. Lett.* **2012**, 109, 107602.
[6] R. Guo, L. E. Cross, S-E. Park, B. Noheda, D. E. Cox and a. G. Shirane, *Phys. Rev. Lett.* **2000**, 84, 5423.
[7] X. Wang, J. Wu, D. Xiao, J. Zhu, X. Cheng, T. Zheng, B. Zhang and X. Lou, *J. Am. Chem. Soc.* **2014**, 136, 2905.
[8] N. Zhang, H. Yokota, A. M. Glazer, Z. Ren, D. A. Keen, D. S. Keeble, P. A. Thomas and Z. G. Ye, *Nat. Commun.* **2014**, 5, 5231.
[9] R. J. Zeches, M. D. Rossell, J. X. Zhang, A. J. Hatt, Q. He, C. H. Yang, A. Kumar, C. H. Wang, A. Melville, C. Adamo, G. Sheng, Y. H. Chu, J. F. Ihlefeld, R. Erni, C. Ederer, V. Gopalan, L. Q. Chen, D. G. Schlom, N. A. Spaldin, L. W. Martin, R. Ramesh, *Science* **2009**, 326, 977.
[10] D. Sando, A. Barthelemy, M. Bibes, *J. Phys.: Condens. Matter* **2014**, 26, 473201. [11] Y. Dai, X. Zhang and G. Zhou, *Appl. Phys. Lett.* **2007**, 90, 262903.
[12] K. Wang and J.-F. Li, *Adv. Funct. Mater.* **2010**, 20, 1924.
[13] S. Zhang, R. Xia, H. Hao, H. Liu and T. R. Shrout, *Appl. Phys. Lett.*,**2008**, 92, 152904.
[14] E. Hollenstein, D. Damjanovic and N. Setter, *J. Eur. Ceram. Soc.* **2007**, 27, 4093.
[15] E. K. Akdoğan, K. Kerman, M. Abazari and A. Safari, *Appl. Phys. Lett.* **2008**, 92, 112908.
[16] D. Xue, Y. Zhou, H. Bao, C. Zhou, J. Gao and X. Ren, *J. Appl. Phys.* **2011**, 109, 054110.
[17] R. Wang, K. Wang, F.-Z. Yao, J.-F. Li, F. H. Schader, K. G. Webber, W. Jo and J. Rödel, *J. Am. Ceram. Soc.* **2015**, DOI: 10.1111/jace.13604.
[18] S. Prosandeev, D. Wang, A. R. Akbarzadeh, B. Dkhil and L. Bellaiche, *Phys. Rev. Lett.* **2013**, 110, 207601.

[19] K. Wang and J.-F. Li, *Appl. Phys. Lett.* **2007**, 91, 262902.
[20] K. Wang, F.-Z. Yao, W. Jo, D. Gobeljic, V. V. Shvartsman, D. C. Lupascu, J.-F. Li and J. Rödel, *Adv. Funct. Mater.* **2013**, 23, 4079.
[21] K. A. Schönau, L. A. Schmitt, M. Knapp, H. Fuess, R.- A. Eichel, H. Kungl and M. J. Hoffmann, *Phys. Rev. B* **2007**, 75, 184117.
[22] S. Wada, K. Yako, H. Kakemoto, T. Tsurumi and T. Kiguchi, *J. Appl. Phys.* **2005**, 98, 014109.
[23] G. A. Rossetti, A. G. Khachaturyan, G. Akcay and Y. Ni, *J. Appl. Phys.* **2008**, 103, 114113.
[24] D. Damjanovic, *J. Am. Ceram. Soc.* **2005**, 88, 2663.
[25] T. R. Shrout, S. J. Zhang, *J. Electroceram.* **2007**, 19, 111.
[26] R. Zuo, T. Granzow, D. C. Lupascu, J. Rödel, *J. Am. Ceram. Soc.* **2007**, 90, 1101.
[27]S.-E. Park, T. R. Shrout, *J. Appl. Phys.* 1997, 82, 1804.
[28] L.-F. Zhu, B.-P. Zhang, L. Zhao and J.-F. Li, *J. Mater. Chem. C* **2014**, 2, 4764.
[29] S.-T. Zhang, A. B. Kounga, E. Aulbach, W. Jo, T. Granzow, H. Ehrenberg and J. Rödel, *J. Appl. Phys.* **2008**, 103, 034108.
[30] D. Wang, Y. Fotinich and G. P. Carman, *J. Appl. Phys.* **1998**, 83, 5342.
[31] F. Chen, Y.-H. Li, G.-Y. Gao, F.-Z. Yao, K. Wang, J.-F. Li, X.-L. Li, X.-Y. Gao and W. Wu, *J. Am. Ceram. Soc.* **2015**, DOI: 10.1111/jace.13461.
[32] S. Lu, Z. Xu, K. W. Kwok and H. L. W. Chan, *Appl. Phys. Lett.* **2014**, 105, 042904.
[33] W. Jo, R. Dittmer, M. Acosta, J. Zang, C. Groh, E. Sapper, K. Wang and J. Rödel, *J. Electroceram.* **2012**, 29, 71.
[34] W. Merz, *Phys. Rev.* **1953**, 91, 513.
[35]A. J. Bell, *Appl. Phys. Lett.* **2000**, 76, 109.
[36]D. J. Franzbach, B.-X. Xu, R. Mueller, K. G. Webber, *Appl. Phys. Lett.* **2011**, 99, 162903.
[37] C. Luo, Y. Wang, Z. Wang, W. Ge, J. Li, H. Luo and D. Viehland, *Appl. Phys. Lett.* **2014**, 105, 232901.
[38]J. Attia, L. Bellaiche, P. Gemeiner, B. Dkhil, B. Malic, *J. Phys. IV France* **2005**, 128, 55.
[39] M. Hinterstein, J. Rouquette, J. Haines, Ph. Papet, M. Knapp, J. Glaum and H. Fuess, *Phys. Rev. Lett.* **2011**, 107, 077602.
[40] J. L. Jones, E. Aksel, G. Tutuncu, T. Usher, J. Chen, X. Xing and A. J. Studer, *Phys. Rev. B* **2012**, 86, 024104.
[41] Y. Qin, J. Zhang, W. Yao, C. Wang and S. Zhang, *J. Am. Ceram. Soc.* **2014**, 98, 1027.
[42] L. Zheng, S. Li, S. Sang, J. Wang, X. Huo, R. Wang, Z. Yuan and W. Cao, *Appl. Phys. Lett.* **2014**, 105, 212902.
[43] A. Pramanick, M. R. V. Jørgensen, S. O. Diallo, A. D. Christianson, J. A. Fernandez-Baca, C. Hoffmann, X. Wang, S. Lan and X.-L. Wang, *Adv. Mater.* **2015**, DOI: 10.1002/adma.201501274.
[44] X. Tan, J. Frederick, C. Ma, W. Jo and J. Rödel, *Phys. Rev. Lett.* **2010**, 105, 255702.
[45] M. Ahart, M. Somayazulu, R. E. Cohen, P. Ganesh, P. Dera, H. K. Mao, R. J. Hemley, Y. Ren, P. Liermann and Z. Wu, *Nature* **2008**, 451, 545.
[46] G. Kresse and J. Furthmüller, *Phys. Rev. B* **1996**, 54, 11169.
[47] J. P. Perdew, K. Burke and M. Ernzerhof, *Phys. Rev. Lett.* **1996**, 77, 3865.
[48] G. Kresse and J. Furthmüller, *Comput. Mater. Sci.* **1996**, 6, 15.

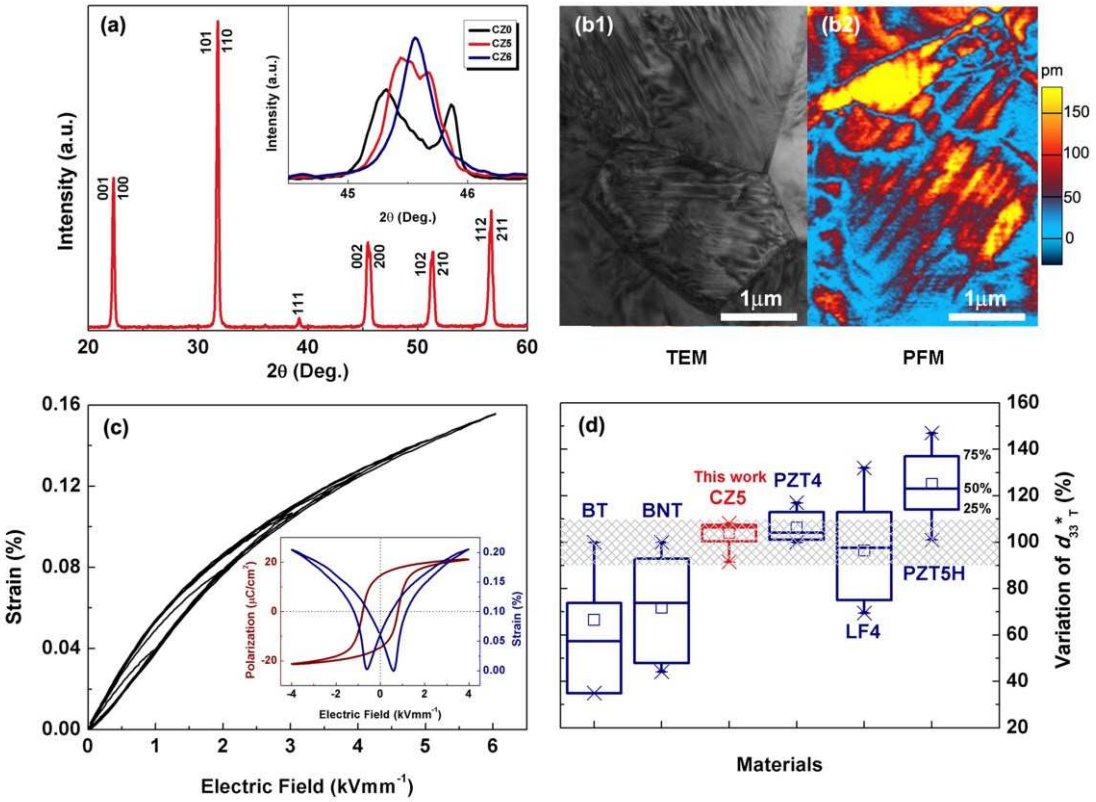

Figure 1. (a) High-resolution X-ray diffraction pattern of CZ5 ceramics at room temperature. An index for tetragonal phase was adopted. The inset is enlarged (002)/(200) peaks of samples with different CZ contents. (b1) TEM and (b2) PFM analysis of typical domain configuration of CZ5 ceramics at room temperature. (c) The unipolar strain versus electric field. The inset is the polarization hysteresis loop and bipolar strain curve at room temperature. (d) Comparison of variation of normalized strain d_{33}* for various piezoceramics as normalized to its room temperature value d_{33}*$_{RT}$ within the temperature range from room temperature up to 140 ^{o}C.

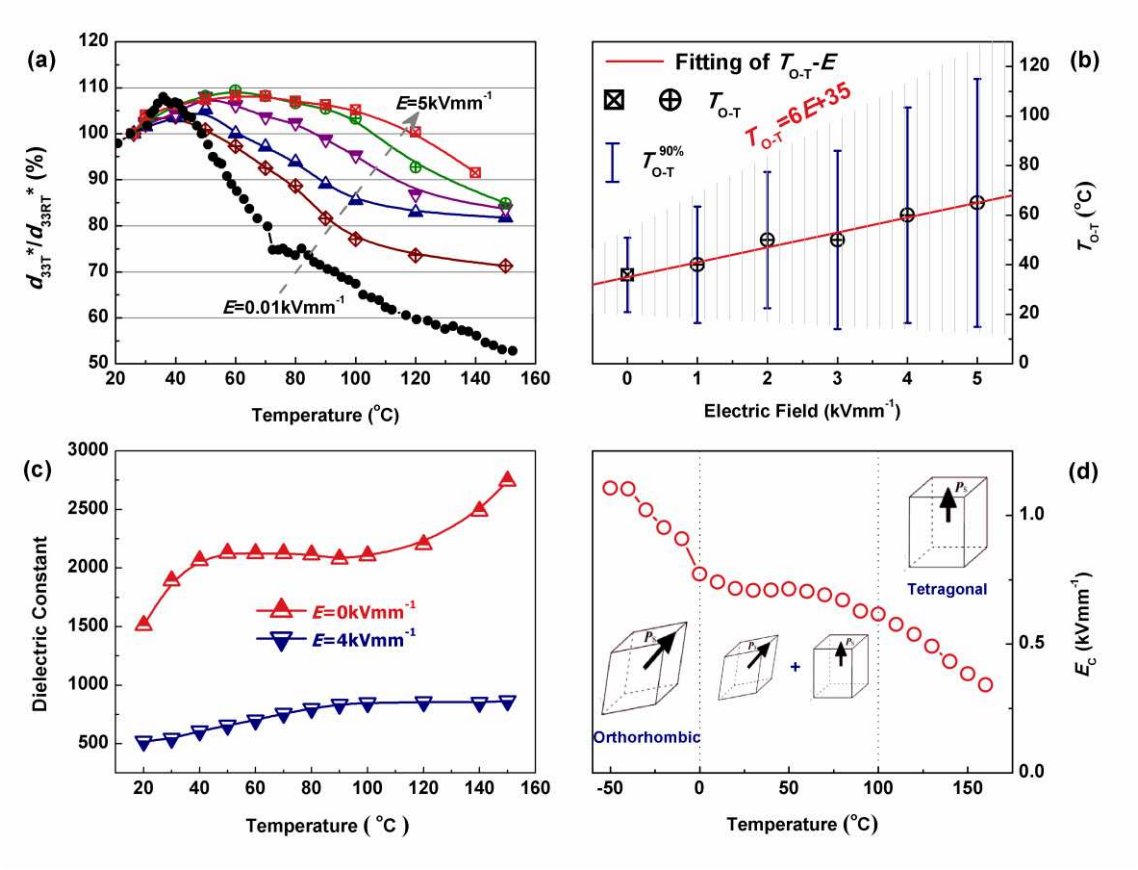

Figure 2. (a) Temperature dependence of d_{33}* normalized to its room temperature value d_{33RT}* of CZ5 ceramics under electric fields ranging from 0.01 to 5 kVmm^{-1}; (b) PPT point T_{O-T} and the range of PPT $T_{O-T}^{90\%}$ as a function of electric field; (c) permittivity curves under electric fields of 0 and 4 kVmm^{-1}; and (d) temperature dependent coercive field E_C.

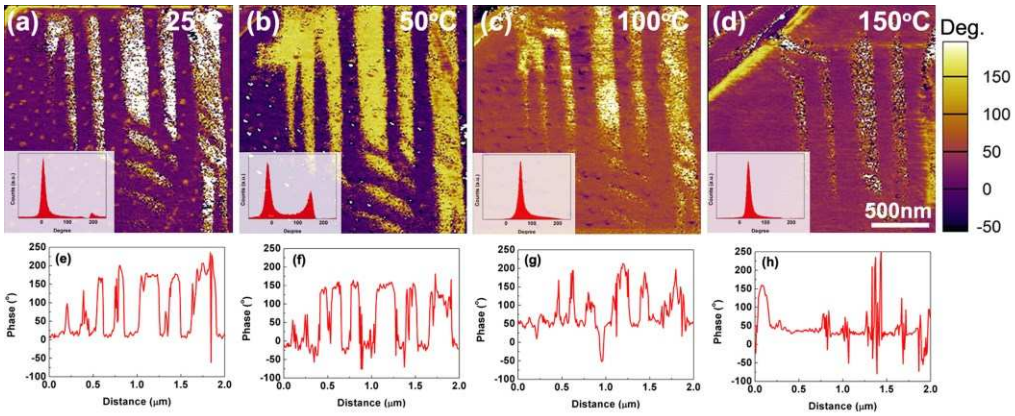

Figure 3. (a-d) Piezoresponse mappings of unpoled CZ5 at temperatures ranging from 25 ^{o}C to 150 ^{o}C with insets showing phase histograms; (e-h) the corresponding piezoresponse phase profiles generated from the line scan across the domains.

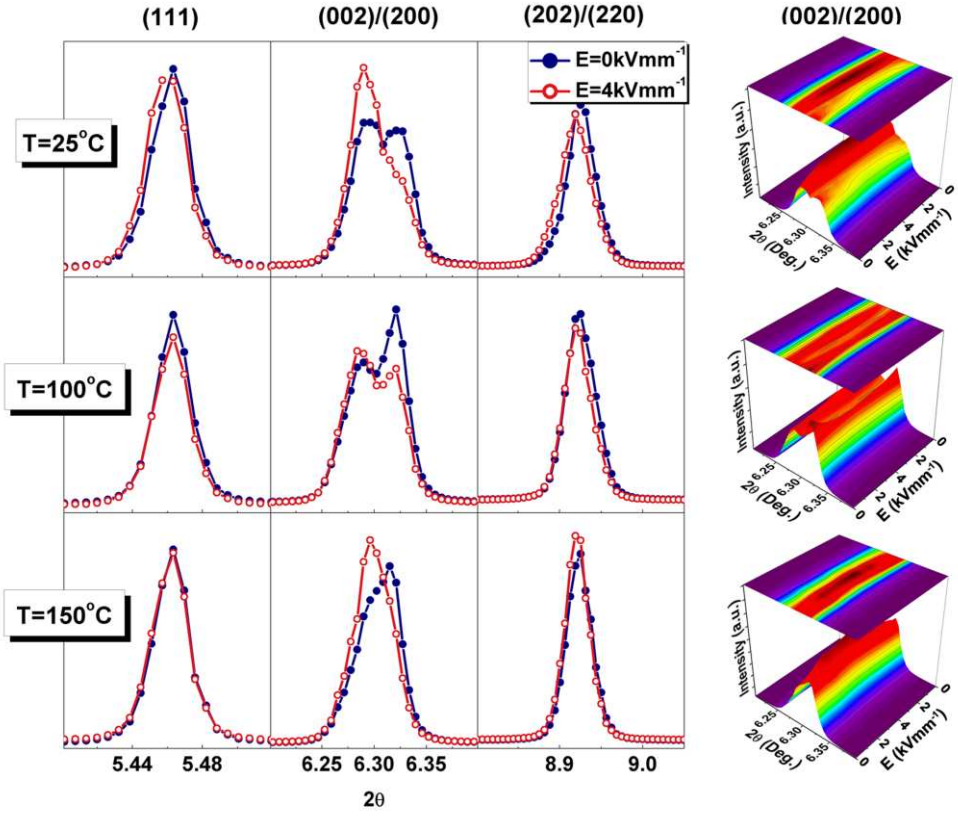

Figure 4. Evolution of *in situ* synchrotron X-ray diffraction profiles for CZ5 ceramics with temperatures and external fields.

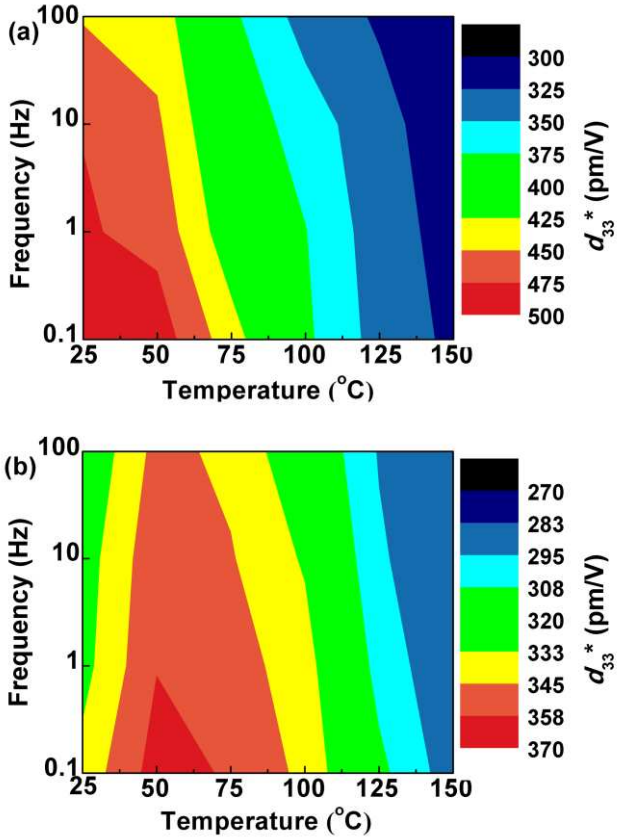

Figure 5. Temperature and frequency dependence of normalized strain d_{33}* of CZ5 ceramics under electric fields of (a) 1 kVmm^{-1} and (b) 4 kVmm^{-1}.

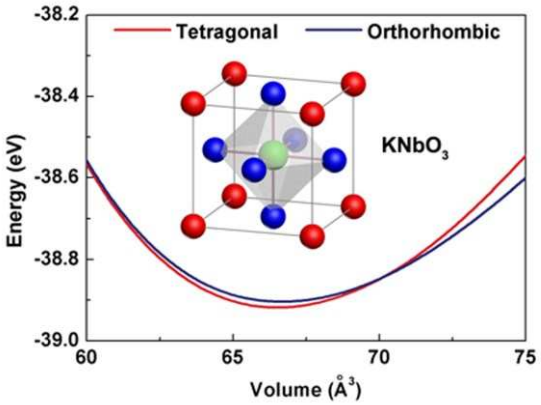

Figure 6. First-principles calculations of the energies of $KNbO_3$ with orthorhombic and tetragonal symmetries. The inset figure illustrates the perovskite structure of $KNbO_3$.

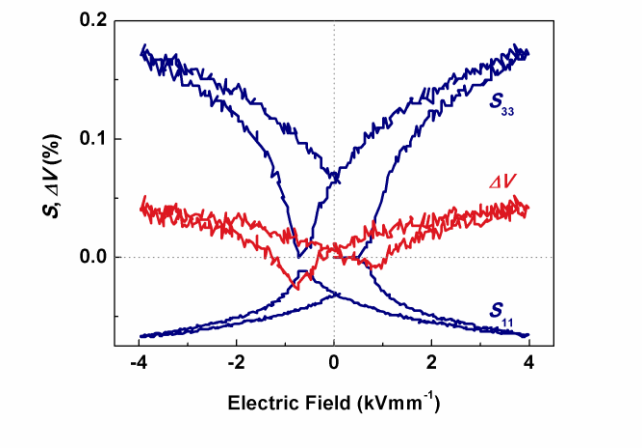

Figure 7. Strain hysteresis with the concurrent volume changes of CZ5 ceramics.

The Table of Contents: A material concept of electrically-enhanced diffused polymorphic phase transition (EED-PPT) is developed to resolve the long-standing issue of temperature-sensitivity in lead-free (K,Na)NbO_3 piezoelectrics. Experimental and theoretical studies reveal that EED-PPT can remarkbaly boost the temperature stability of (K,Na)NbO_3, where the normalized strain d_{33}* almost keeps constant from room temperature up to 140 ^{o}C.

Keyword: lead-free, piezoceramics, diffused phase transition, temperature stability

Authors: Fang-Zhou Yao, Ke Wang,* Wook Jo, Kyle G. Webber, Timothy P. Comyn, Jing-Xuan Ding, Ben Xu, Li-Qian Cheng, Mu-Peng Zheng, Yu-Dong Hou, and Jing-Feng Li*

Title: Diffused Phase Transition Boosts Thermal Stability of High-Performance Lead-Free Piezoelectrics

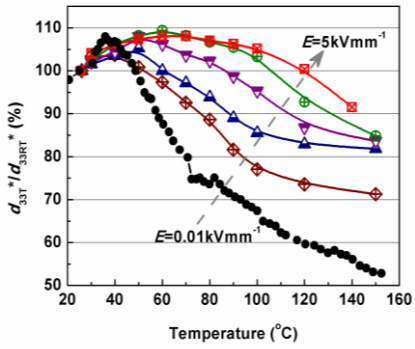

ToC figure